Study of Influence of Operating Parameters on Braking Distance

Tang, Tianchi; Anupam, Kumar; Kasbergen, Cor; Scarpas, Athanasios

DOI
10.3141/2641-16

Publication date
2017

Document Version
Accepted author manuscript

Published in
Transportation Research Record

Citation (APA)
Tang, T., Anupam, K., Kasbergen, C., & Scarpas, A. (2017). Study of Influence of Operating Parameters on Braking Distance. *Transportation Research Record*, *2641*(1), 139-148. Article 2641-16. https://doi.org/10.3141/2641-16

Study of Influence of Operating Parameters on Braking Distance

Tianchi Tang, Corresponding Author
Faculty of Civil Engineering & Geosciences
Delft University of Technology, Stevinweg 1, 2628 CN, Delft, The Netherlands
Tel: +31 15 2784676; Email: t.tang@tudelft.nl

Kumar Anupam
Faculty of Civil Engineering & Geosciences
Delft University of Technology, Stevinweg 1, 2628 CN, Delft, The Netherlands
Tel: +31 15 2782394; Email: k.anupam@tudelft.nl

Cor Kasbergen
Faculty of Civil Engineering & Geosciences
Delft University of Technology, Stevinweg 1, 2628 CN, Delft, The Netherlands
Tel: +31 15 2782729; Fax: +31 15 2785767; Email: c.kasbergen@tudelft.nl

Athanasios Scarpas
Faculty of Civil Engineering & Geosciences
Delft University of Technology, Stevinweg 2, 2628 CN, Delft, The Netherlands
Tel: +31 15 2784017; Fax: +31 15 2783443; Email: a.scarpas@tudelft.nl

Word count: 4724 words text + 11 tables/figures x 250 words (each) = 7474 words

TRR Paper number: 17-02602

February 2017

ABSTRACT
Stopping distance includes the driver thinking distance and braking distance. Braking distance is one of the basic standards for road design and maintenance practices. Adequate tire-pavement skid resistance plays a significant role in reducing the braking distance and consequentially enhancing road driving safety conditions. With modern technology such as the anti-lock braking system (ABS), the friction force is maximized by controlling the brakes on and off repeatedly such that the braking distance is shortened. Several previous studies have shown the effect of some parameters, such as water film thickness, tire inflation pressure and wheel load on the braking distance. But relatively less discussion is about the effect of the slip ratio, temperature, and pavement surface characteristics. Measuring the braking distance in the field is energy- and time consuming apart from the uncertainties in the environmental conditions. General approaches to calculate the braking distance are based on basic mechanics principles. To the author's knowledge, a model capable of simulating the whole braking process is not yet available. In the current study, a way to predict braking distance by means of finite element (FE) modelling only is proposed. A model capable of including the effect of parameters such as temperature, slip ratio and asphalt surface characteristics on the braking distance is introduced.

INTRODUCTION

Adequate stopping distance is of great importance for road safety. Typically, the stopping distance contains two parts, namely reaction distance and braking distance *(1)*. Reaction distance depends mainly on factors such as the driver's attention, vision**,** and perception *(2)*. Stopping distance is affected by both vehicular and environmental conditions, such as brakes, tires, vehicle weight, vehicle age, road surface, road gradient and weather *(3)*. The skid resistance which is represented by the skid resistance coefficient between the pavement and the tire is the key parameter that can influence braking distance *(4)*.

Braking distance is one of the basic standards for road design and maintenance practices. The braking distance required for safety varies with different pavement surface textures. This variation is attributed to the fact that skid resistance varies from one surface to another. At low speed, microtexture is the main contribution to skid resistance, while at a high-speed macrotexture is the main contribution *(5)*. Liu *(6)* found that macrotexture parameters of the road surface, namely the aggregate size and the gap width had considerable influence on the values of skid resistance.

Generally, the braking distance of wet pavement is relatively longer than that of dry pavement. Past studies show that the number of accidents on wet pavements is twice as high as compared to dry pavements *(7)*. In general, the braking distance increases with increasing speed and increasing water film thickness at a full braking operation (100% slip) *(8)*.

Temperature is another important factor that influences the braking distance. The change of the skid resistance due to temperature change results in the change of the braking distance of the vehicle. Jayawickrama and Thomas *(9)* observed that skid resistance is typically higher in winter than in summer *(9)*. The skid resistance of a given surface is a function of the pavement temperature, and normally, the higher the pavement temperature is, the lower the skid resistance will be*(10)*. The frictional properties of the pavement are also highly influenced by the ambient temperature *(11)*. Saito and Henry *(12)* found that there is a high correlation between air temperature, tire temperature, and pavement temperature.

Experimental studies have shown that the coefficient of skid resistance for a road surface usually peaks between 10% and 20% slip ratio *(13)*. An anti-lock braking system (ABS), which is nowadays available to most of the motor cars, is capable of keeping the slip ratio within the peak range while braking. The peak coefficient is twice the sliding coefficient which implies the important effect of the slip ratio on skid resistance*(14)*. The above discussions highlight the importance of maintaining peak slip ratio on the braking distance.

Several numerical and field studies on braking performance have been conducted *(16, 17, 27)*. However, in most of the numerical studies, the skid resistance during whole braking operation is assumed to be constant, with assumption such as the angular speed of the tire decreases linearly. Researchers *(18)* have highlighted that this assumption may not be correct due to the fact that the skid resistance varies with speed, and as such during the whole braking process, it will not be constant. An analytical simulation model to evaluate the characteristics of tire–pavement skid resistance behavior was introduced in the previous study *(19)*. It proposed a two-step approach to evaluate the braking distance by post-processing the data of FE analyses and kinematics equations. However, this model neglects the effect of real pavement texture and slip conditions. Researchers have shown that the skid resistance prediction and thus the braking distance prediction by finite element model can be significantly improved if the effect of surface texture is brought into the model *(14)*.

The extreme dense mesh for pavement surface which contains millions of elements makes it currently infeasible with current computational capabilities to simulate the whole

braking process in one go. In this paper, a methodology is presented to predict braking distance directly from the model itself without the need of post processed data. This model is capable of simulating tire geometry characteristics, pavement surface asperities, and tire operating parameters. The advantage of this model is that it allows one to simulate a braking vehicle where mass and inertia of the wheel can also be taken into account. This will provide an easy and reliable tool for road engineers to evaluate the braking distance for pavement design & performance prediction purposes.

In this paper, a tire-pavement interaction model is developed to study the effects of various parameters on the braking distance. The following parameters are considered as inputs in this study:

- Wheel load, inflation pressure, and initial speed;
- Ambient and pavement temperature;
- Water film thickness;
- Tire type;
- Slip ratio;
- Asphalt surface macrotextures.

The developed model automatically calculates the hysteresis component of friction whereas the adhesion component is provided as an input value. The simulation procedure involves a 3D FE tire traversing on an asphalt mesh. A PIARC (World Road Association) 165R15 (25) and a Goodyear patterned tire with vertical tire load in a range of 3000 N- 4000 N, tire inflation pressure in a range of 150-250 kPa, translational speed in a range of 40-150 km/h, and two slip ratios of 20% and 100% were parametrically studied. Four asphalt pavement surfaces, namely porous asphalt (PA), ultrathin surface (UTS), sand asphalt (SA) and dense asphalt concrete (DAC-10) were utilized. The conditions of ambient temperature (AT) and pavement temperature (PT) both ranging from 10°C to 50°C were applied to study the temperature effect. Two water film thicknesses of 2.5 mm and 5 mm respectively were also investigated.

DESCRIPTION OF THE FE MODEL

The simulation was conducted using the commercial software Abaqus 6.13 *(20)* and an in-house Fortran program. The detailed procedure of the development of the tire-pavement interaction model is discussed in the previous works *(14, 21, 22)*. However, for the ease of the readers' understanding, a brief description is presented in this section. The FE meshes of the pavement surfaces are obtained by scanning the samples of selected pavement types by using an X-ray tomographer and the ScanIP software *(23)*. The material properties of the tire rubber are obtained by laboratory tests and are taken as the input parameters in the model. The calculation of the skid resistance coefficient is based on the energy dissipation at each Gauss point of all the tire cross-section elements, which can be expressed as follows:

$$\Delta W_v = \int_0^T S_e : L_v dt \quad (1)$$

where

ΔW_v=dissipation loss per unit volume per cycle,

S_e=second Piola–Kirchhoff tensor,

L_v=spatial velocity gradient tensor,

T= total time,

dt= time increment and

symbol ":" denotes the "double dot operation"

The rate of the heat generation $\dot{Q}$ are estimated using Equation (1) as follows:

$$\dot{Q} = \frac{\Delta W_v}{T} = \frac{1}{T}\sum_{m=1}^{M}\sum_{k=1}^{K}\int_{m=1}^{M} S_e^{km} : L_v^{km} dt \quad (2)$$

where k = 1, 2, . . . , K represents the number of the sections in the 3D tire model and m = 1, 2, . . . , M represents the number of elements in each section of the 3D tire model. The heat generation rates obtained from Equation (2) act as an input to heat transfer analysis. Thermal analysis is carried out on the two-dimensional FE mesh which is of the same mesh density as that of the tire model. The nodal temperatures are then calculated based on the conductive and convective thermal coefficient of the tire rubber. The tire material properties are updated with the new temperature development in the tire cross section, and the process is repeated until the predicted temperature is converged. The hysteretic friction of the tire is computed as an output depending on the new material properties.

In order to validate the capability of the model to predict the friction coefficient, data measured by a French friction testing device called Adhera (*15*) was used. The field experiments were performed on the IFSTTAR (French Institute of Science and Technology for Transport, Development, and Networks) test tracks at various speeds. Figure 1 shows the comparison between the experimental and the model predicted braking distance for a locked PIARC tire on a PA surface at three different speeds: 40 km/h, 60 km/h, and 90 km/h. The braking distances are calculated from the friction measurements. It should be noted that readers can refer to the authors' previous works *(14,15)* for details on this validation process.

The overall framework is shown in Figure 2. In order to calculate the breaking distance following steps are followed:

1. As a first step of the modeling, the discretized 3D FE model of the tire is created on the basis of its 2D cross-sectional geometry. Subsequently, the tire footprint and the steady state rolling analysis is carried out on a plane pavement surface, as shown in Figure 2.
2. The morphologies of the asphalt pavement surfaces are introduced by replacing plane pavement mesh with the mesh of real surface scans, as shown in Step 3 of Figure 2. The developed stresses and deformation history from the previous step of static analyses is retained and transferred to the next phase of transient analysis. During this phase of analysis, the tire is rolled/skidded over the desired asphalt surface mesh and the Fluid elements are added to simulate the wet condition. At any prescribed speed, the skid resistance coefficient is calculated with the procedure as described earlier.
3. From a prescribed maximum speed, the speed is gradually reduced in smaller steps to a prescribed lower limit by repeating the above-mentioned steps. In this study, the maximum and minimum speed limits are set at 150 and 20 km/h respectively. A relationship between the coefficient of friction and the speed is obtained which acts as an input to the final Step 5.
4. As mentioned, due to dense FE meshes it is nearly impossible to perform whole breaking simulation on a surface with morphologies. Therefore, the breaking distance simulation which requires a significant length of the pavement mesh is carried out on the plane pavement surface which is already developed in Step 2. The tire is prescribed with maximum speed at t=0, whereas the pavement surface is provided with the friction law according to the earlier obtained friction-speed relationship. The simulation is carried out till the tire has nearly zero speed (t=t_s) and thus breaking distance is obtained.

RESULTS AND DISCUSSIONS

As discussed previously, the braking distance is influenced by many factors. In this section, these affecting factors i.e. wheel load, inflation pressure, ambient and pavement temperature, road surface characteristics, water film thickness and tire type are studied respectively. Following that, a comparison of the Euro standard *(25)* and AASHTO *(26)* is presented. Findings and discussions are shown in each corresponding subsection.

Influence of Speed on Braking Distance

The effect of vehicle speed on the braking distance with an axle load of 4000 N and inflation pressure of 150 kPa is shown in Figure 3. The plots show that the braking distances increase with the vehicle speed, however, their rates of increment depends on the slipping condition of the vehicle. For example, for 100% slip the braking distance increases by 160 m from 10 m at the speed of 40km/h to 170m at the speed of 120 km/h. On the other hand, an increment of 90 m is observed for 20% slip with the same change in speed. The increments of the braking distance with speed are mainly due to more amount of the work required to stop the car. This is in line with the findings of previous studies *(18)*.

Influence of Wheel Load on Braking Distance

The effect of wheel load on the braking distance is shown in Figure 4. As a common basis for comparison, an SA pavement surface, a constant inflation pressure of 150 kPa, a speed of 40 km/h, and an ambient temperature of 40°C were considered. Wheel loads ranging from 3000 to 4000 N were considered. The plots show that the braking distance decreases with the increase of the wheel load. This can be attributed to the increase of the energy dissipation due to the larger deformation of the tire. The increase in the computed braking friction coefficients was observed to be 4 m and 10 m for the slip ratios of 20% and 100% slip ratios, respectively, for a change of load from 3000 to 5000 N. This result suggests that changeable loading conditions have a smaller effect on the braking distance of 20% slipping wheel than a locked wheel.

Influence of Inflation Pressure on Braking Distance

The effect of inflation pressure on the braking distance is shown in Figure 5. For the evaluation of the relative interaction of braking distance against inflation pressure, 150 to 250 kPa were considered. For this pressure range, the FE simulations were performed for the tire with a constant load of 4 kN, traversing an SA pavement surface mesh at a speed of 80 km/h. The braking friction values were computed at slip ratios of 20% and 100%. The plot shows that braking distance increases with tire inflation pressure. This effect is attributed to the increase in the pressure inflated and leads to a decrease of contact surface which reduces the braking force. The effect of tire inflation pressure on braking distance is more pronounced for a locked wheel than for a slipping wheel. For instance, the percentage decrease in braking distance was observed to be 7% and 27% for slip ratios of 20% and 100%, respectively, when the tire inflation pressure changed from 150 to 250 kPa.

Influence of Ambient and Pavement Temperatures on Braking Distance

The effect of ambient and pavement temperatures on the braking distance is shown in Figure 6. The results show that at constant load, inflation pressure, and speed, the values of braking distance increase with an increase in the pavement and ambient temperatures. For example, for an SA pavement surface, the predicted braking distance increases from 7 m to 8 m for 20% slip ratio and 9 m to 10 m for 100% slip ratio for an increase of ambient temperature from 10°C to 50°C (Figure 6a). An increase of braking distance of from 8 m to 10 m for slip ratios of 20% and 12 m to 15 m for slip ratio of 100% for an increase of pavement

temperature from 10°C to 50°C (Figure 6b). Higher ambient and pavement temperatures increased the overall tire temperature, which lowered the material modulus properties and lowered the braking force.

Influence of Asphalt Mix Design on Braking Distance

The effect of asphalt mix design on the braking distance is shown in Figure 7. Under the same condition, the longest braking distance is on SA surface, followed by DAC-10, UTS, and PA for both slip ratio of 20% and 100%. For example, at the speed of 120 km/h and 100% slip ratio, the braking distance is 169 m for a PA surface and 126 m for an SA surface, showing a decrease of about 25%. At the speed of 120 km/h and 20% slip ratio, the braking distance for a PA surface is 79 m while that for an SA surface is 98 m, showing a decrease of about 20%. The result indicates that an SA surface with a relative smooth macrotexture provides lower skid resistance properties than a surface with a PA mix design. This result is in line with the fact that improved macrotexture provides more skid resistance.

Influence of Water Film Thickness on Braking Distance

The effect of water film thickness on the braking distance is shown in Figure 8. The braking distance against water film is evaluated for water film thickness of 2.5mm and 5mm. The Goodyear patterned tire is considered for the evaluation. The result indicates that with an increase of the water film thickness the braking distance increases accordingly. For example, the plot shows that for a slip ratio of 100% the braking distance is 139 m for water film thickness of 2.5 mm and 185 m for water film thickness of 5 mm at the speed of 150 km/h. In terms of percentage benefits, it means an increase of 32%. Under similar condition but for a peak slip ratio of 20%, the braking distance is 96 m for water film thickness of 2.5 mm and 101 m for water film thickness of 5 mm at the same speed. An increase of 6% is observed. The results are attributed to the fact that the wet skid resistance decreases with the increase of the water film thickness *(24)*. The 20% slip braking shows a much safer operation as compared with the 100% braking.

Influence of Tire Types on Braking Distance in Wet Weather Condition

The effect of tire type on the braking distance in wet weather condition is shown in Figure 9. A Goodyear patterned tire and a PIARC smooth tire are considered in the simulation with a water film thickness of 7.5mm. The result indicates that a properly grooved tire will result in a lesser braking distance compared with a worn-out tire in wet condition. For instance, for a slip ratio of 20%, the braking distance is 96 m for a smooth tire and 79m for a patterned tire at the speed of 120 km/h i.e. a decrease of 18% in breaking distance. While for a slip ratio of 100%, the braking distance is 227m for a patterned tire and 134 m for a smooth tire at the same speed i.e. a decrease of 40% is observed. This result is attributed to low wet friction values with the smooth tire in the wet weather condition. It also implies that a proper tire design with proper grooves will lower accidents in wet weather. The results can be utilized by highway agencies and authorities to identify and set upper and lower limit safety boundaries, which in turn may help them to take adequate measures in terms of the speed limit, safe vehicle distance etc .

Euro and AASHTO Standard on Stopping Distance

The comparison on stopping distance with the Euro standard *(25)* and AASHTO *(26)* is shown in Figure 10. The minimum stopping distances specified by both of the standards are shown in Table 1. The Euro standard does not specify detailed braking distance computation formulas. In AASHTO, the stopping distance can be calculated using the following formula:

$$\text{stopping distance} = 0.695v + 0.039\,\frac{v^2}{a}$$

where v is the speed of the vehicle (km/h) and a is the acceleration set to 3.4 m/s^2.

The reaction time assumed in the calculation is 2.5s. Four asphalt pavement surfaces are considered in the comparison. The plot shows that at a relatively low speed (<80 km/h), all the asphalt mix surfaces fulfill both of the standards. However, at a relatively high speed (>110 km/h), all the asphalt mix surfaces fulfill AASHTO but only the stopping distance for PA pavement surface meets the Euro standard. This scenario shows that for highway design, the pavement with open graded mix design should be preferred over other mix designs. Furthermore, the results may also provide the transportation agencies with one basis for the establishment and improvement of road design standard.

CONCLUSIONS

This paper presents a calibrated model using FE numerical approach to evaluate the braking distance under various operating conditions such as different slip ratios and environmental conditions such as different surrounding temperatures. In conclusion, it can be said that the developed FE model could satisfactorily estimate the braking distance under prescribed conditions and is an effective means to study the influences of various factors on braking distance without the need for large-scale experiments. The study highlights the importance of including the different tire characteristics and pavement characteristics as well as different environmental factors into the currently used road safety criteria. The model could be utilized by the researchers to gain a deeper insight into the mechanism of the tire-pavement interaction during the process of braking. On the other hand, road researchers could also use such models even in the mix-level design to judge the performance of innovative mixes with respect to its braking performances. Furthermore, it could also be used in the pavement management system (PMS) to identify intervention levels.

In general, results show that the braking distance increases with the increase of vehicle speed , and surrounding temperatures. Results also indicate that during an emergency a fully locked wheel will result in a longer braking distance as compared with a partially locked wheel, which indicates a more dangerous situation. The paper also highlights the importance of maintaining proper grooving in the tire. A tire with sufficient groove depths offers a shorter braking distance than a worn-out tire. It is also important for a driver to maintain sufficient tire inflation pressure, as the lower inflated tire will lead to a longer braking distance.

The simulation was carried out considering four different pavement surfaces namely PA, UTS, DAC-10, and SA surfaces. It was found that PA pavement surfaces offer the shortest braking distance, followed by UTS, DAC-10, and SA. Similarly, wet surface offers a longer braking distance comparing with a dry surface as the water film reduces the skid resistance between the tire-pavement interface.

REFERENCES

1. *NCHRP Report 400: Determination of Stopping Sight Distances.* National Cooperative Highway Research Program. Transportation Research Board (National Academy Press). ISBN 0-309-06073-7, 1997.
2. Taoka, and George T. Brake Reaction Times of Unalerted Drivers. *ITE Journal*, Vol. 59(3), 1989, pp. 19–21.
3. Layton R., and Karen D. Stopping Sight Distance. The Kiewit Center for Infrastructure and Transportation, USA, 2012. http://cce.oregonstate.edu/sites/cce.oregonstate.edu/files/12-2-stopping-sight-distance.pdf. Accessed Jul. 25, 2016.

4. J. J. Henry. *Comparison of the Friction Performance of a Passenger Car Tire and the ASTM Standard Test Tires*. Special Technical Publication 793, ASTM, Philadelphia, Pa., 1983, pp. 219-231
5. Shaffi, M.A.B. *Skid Resistance and the Effect of Temperature*. University of Teknologi, Johor Bahru, Malaysia, 2009.
6. Liu, Y.R., Fwa, T.F., and Choo, Y.S. Effect of Surface Macrotexture on Skid Resistance Measurement by the British Pendulum Test. *Journal of Testing and Evaluation*, Vol. 32, No.4, 2004, pp. 304-309.
7. Jonathan, L.L. *The Effect of Pavement Skid Resistance on Wet Pavement Accidents in Indiana*. Purdue University and Indiana State of Highway Commission, 1977. http://docs.lib.purdue.edu/cgi/viewcontent.cgi?article=2290&context=jtrp. Accessed Jul.25, 2016
8. H. R. Pasindu, T. F. Fwa, and G. P. Ong. Computation of Aircraft Braking Distances. *Transportation Research Record: Journal of the Transportation Research Board*, No. 2214, 2011, pp. 126–135.
9. Jayawickrama, P. W., and B. Thomas. Correction of Field Skid Measurements for Seasonal Variation in Texas. *Transportation Research Record: Journal of the Transportation Research Board*, No. 1639, 1998, pp. 147–154.
10. Sigit, P.H., Eky, S.S. and Husnul, F. The influence of Buton Asphalt Additive on Skid Resistance Based on Penetration Index and Temperature. *Construction and Building Material*, Vol. 42, 2013, pp. 5-10.
11. M.A. Khasawneh, and R.Y. Liang. Temperature Effect on Frictional Properties of HMA at Different Polishing Stages. *Jordan Journal of Civil Engineering*, Vol. 6(1), 2012, pp. 39-53.
12. Saito, K, and J. J. Henry. Mechanistic Model for Predicting Seasonal Variations in Skid Resistance. *Transportation Research Record*, No. 946, 1983, pp. 29–38.
13. Henry, J. J. *NCHRP Synthesis of Highway Practice 291: Evaluation of Pavement Friction Characteristics*. TRB, National Research Council, Washington, D.C., 2000.
14. S.K. Srirangam, K. Anupam, C. Kasbergen, and A. Scarpas. Study of Influence of Operating Parameters on Braking Friction and Rolling Resistance. *Transportation Research Record: Journal of the Transportation Research Board*, No. 2525, 2015, pp. 79–90.
15. Anupam, K., S. K. Srirangam, A. Scarpas, C. Kasbergen, and M. Kane. Study of Cornering Maneuvers of a Pneumatic Tire on Asphalt Pavement Surfaces Using the Finite Element Method. *Transportation Research Record: Journal of the Transportation Research Board*, No. 2457, 2014, pp. 129–139.
16. W.G Zhang, J. Yang, and L. Cong. The Effect of Asphalt Pavement Texture on Braking Distance. Submitted for 3rd International Conference on Road Safety and Simulation, Indianapolis, USA, 2011.
17. M. Grujicic, W.C. Bell, G. Arakere, and I. Haque. Finite Element Analysis of the Effect of Up-armoring on the Off-road Braking and Sharp-turn Performance of a High-Mobility Multi-purpose Wheeled Vehicle (HMMWV). *Journal of Automobile Engineering*, Vol. 223(D11), 2009, pp. 1419-1434.
18. R.L. Rizenburgs. Discussion on Skid Resistance of Pavement Surfaces. Kentucky Department of Highways, USA, 1968.
19. Ong, G.P. and Fwa, T.F. Mechanistic interpretation of braking distance specifications and pavement friction requirements. *Transportation Research Record: Journal of the Transportation Research Board*, No. 2155, 2010, pp. 145-

157.
20. *ABAQUS User's Manual. Version 6.13*. Dassault Systemes, Vélizy- Villacoublay, France, 2013.
21. Srirangam, S. K., K. Anupam, A. Scarpas, and A. Köster. Influence of Temperature on Tire-Pavement Friction-1: Laboratory Tests and Finite Element Modelling. Presented at 92nd Annual Meeting of the Transportation Research Board, Washington, D.C., 2013.
22. Anupam, K., S. K. Srirangam, A. Scarpas, and C. Kasbergen. Influence of Temperature on Tire–Pavement Friction: Analyses. *Transportation Research Record: Journal of the Transportation Research Board*, No. 2369, 2013, pp. 114–124.
23. SIMPLEWARE. ScanIP 32-bit, Version 4.3. +CAD 32-bit, Version 1.3. 2011.
24. V. Beautru, V. Cerezo, M.T. Do, and M. Kane. Influence of Thin Water Film on Skid Resistance. 7th Symposium on Pavement Surface Characteristics, France, 2012.
25. United Nations Economic Commission for Europe. *European Agreement on Main International Traffic Arteries (AGR).* Geneva, 2002.
26. *A Policy on Geometric Design of Highways and Streets*, 6th ed. AASHTO, Washington D.C., 2010.
27. Liebermann, D. G., G. Ben-David, N. Schweitzer, Y. Apter, and A. Parush. A Field Study on Braking Responses during Driving, I. Triggering and Modulation. *Ergonomics*, Vol. 38, No. 9, 1995, pp. 1894–1902.

LIST OF TABLES

LIST OF FIGURES

TABLE 1 Euro Standard and AASHTO Requirement 2010 for Minimum Stopping Distance

Design speed (km/h)	Minimum stopping distance (m) (Euro standard)	Minimum stopping distance (m) (AASHTO Requirement (2010))
60	70	84
80	100	130
100	150	186
120	200	252

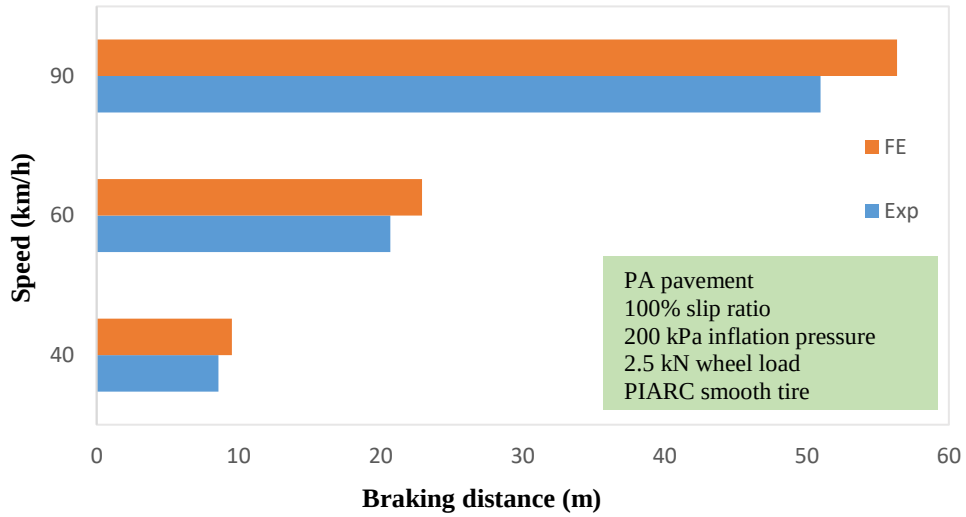

FIGURE 1 Verification of simulation model against experimentally measured data

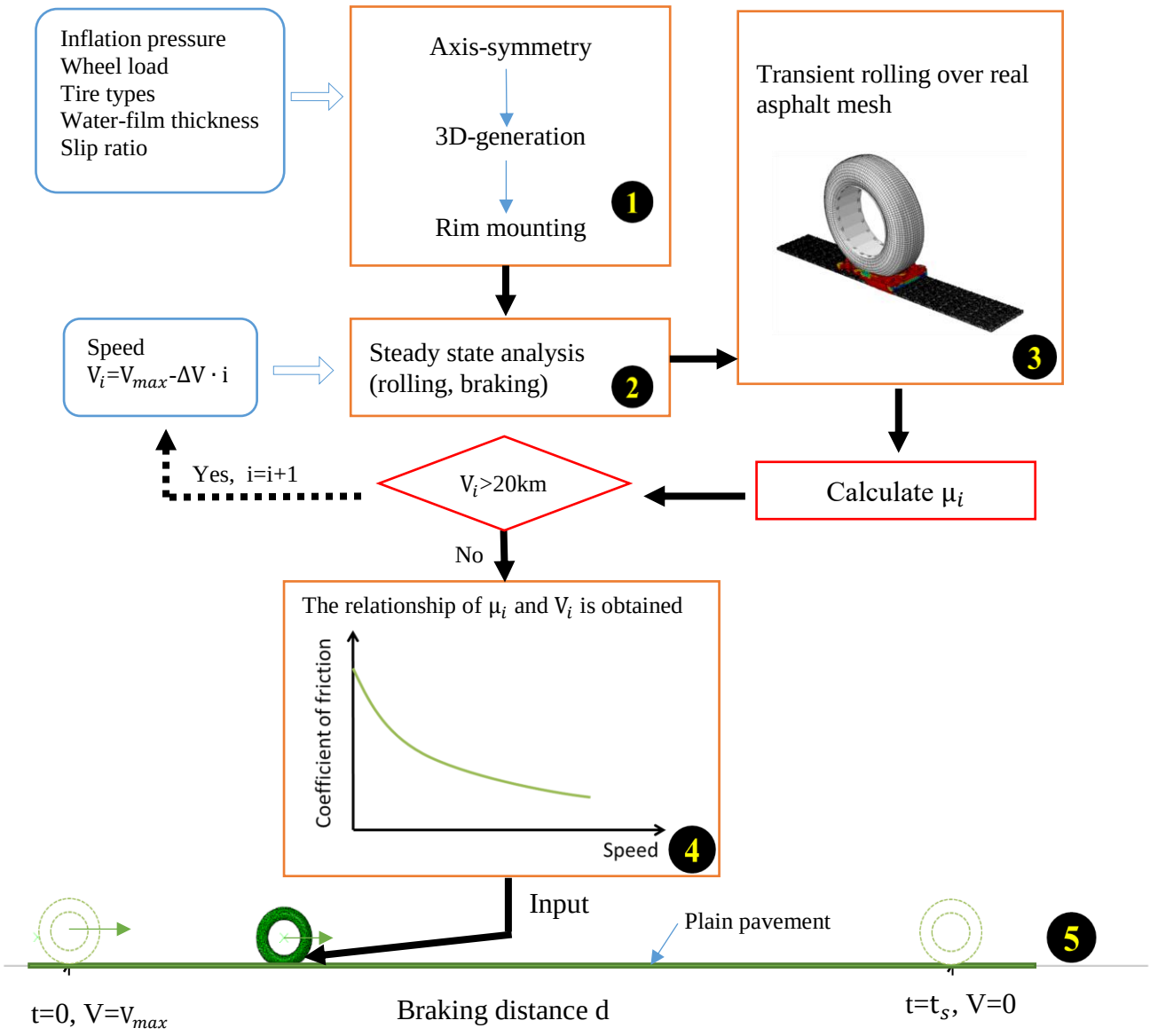

FIGURE 2 Overall framework for the evaluation of braking distance

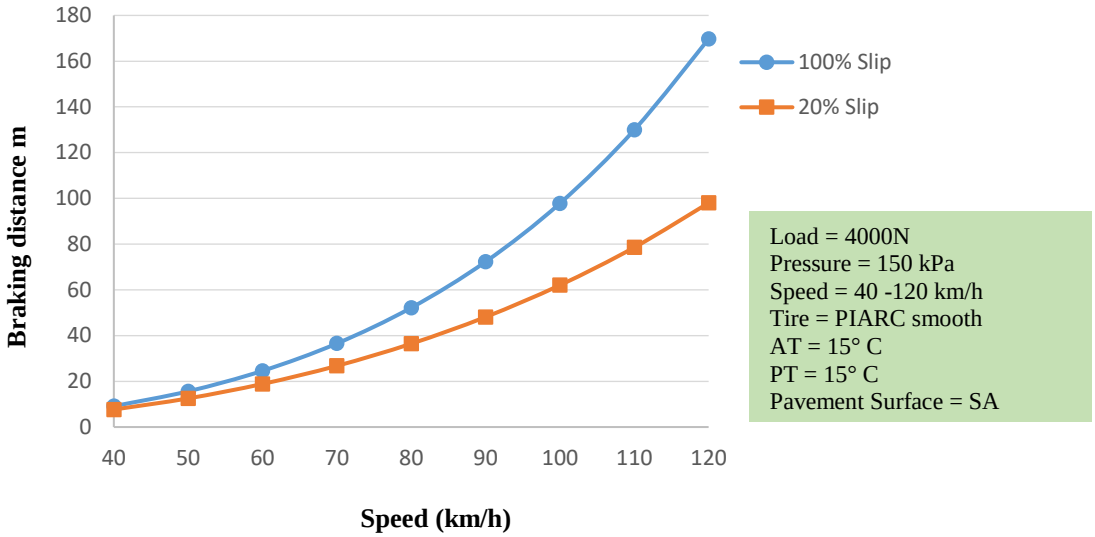

FIGURE 3 Schematic of influence of speed on braking distance

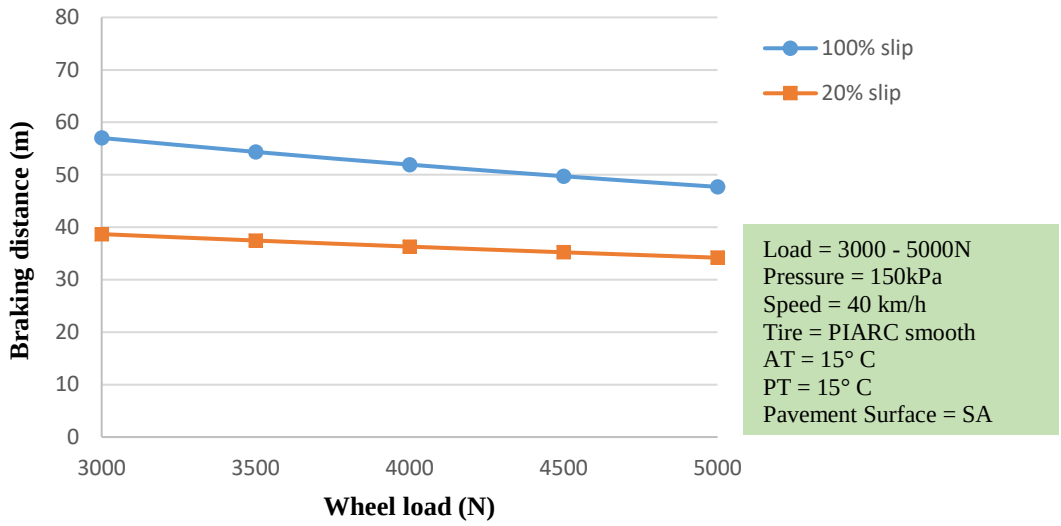

FIGURE 4 Schematic of influence of wheel load on braking distance

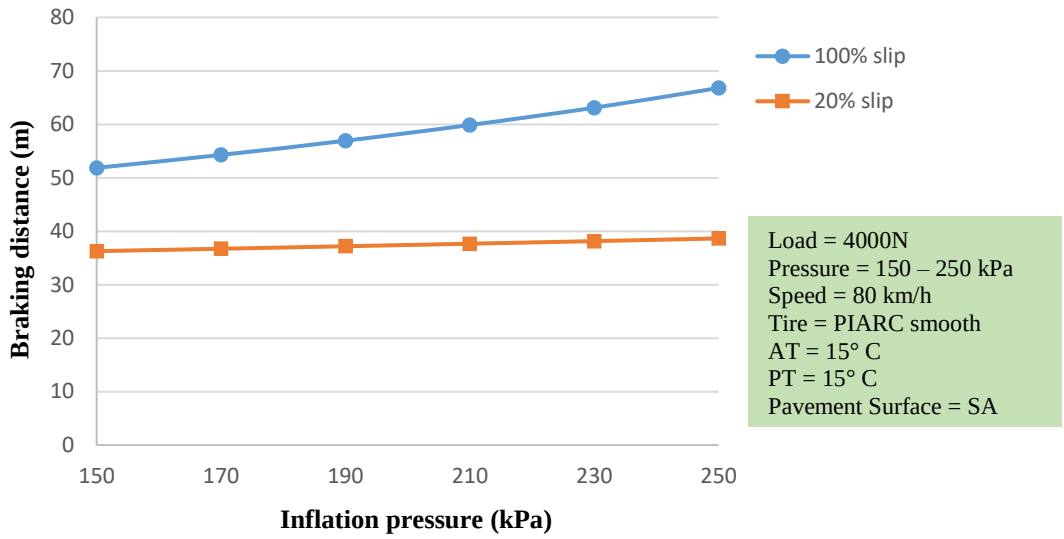

FIGURE 5 Schematic of influence of inflation pressure on braking distance

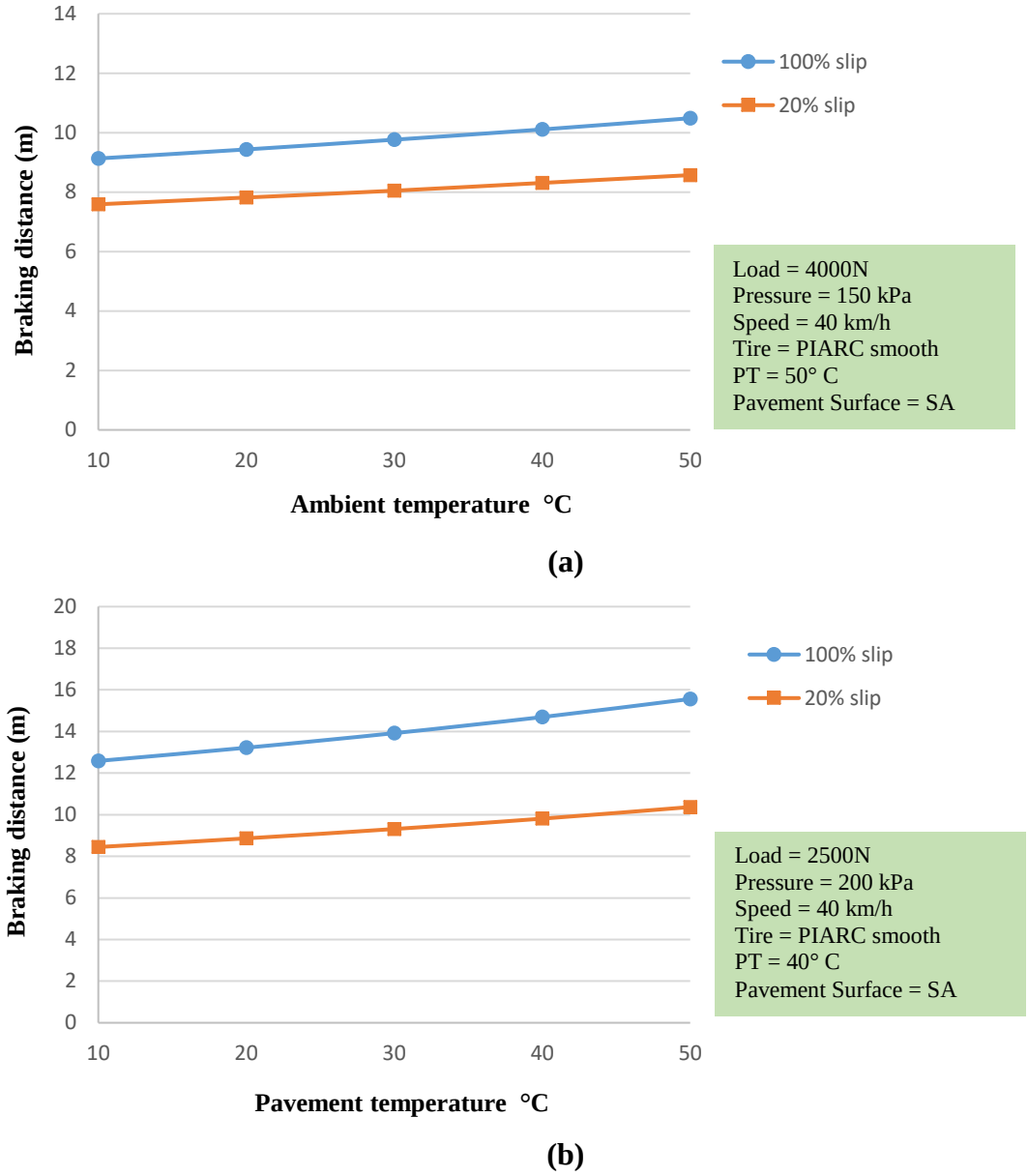

FIGURE 6 Schematic of influence of temperature on braking distance

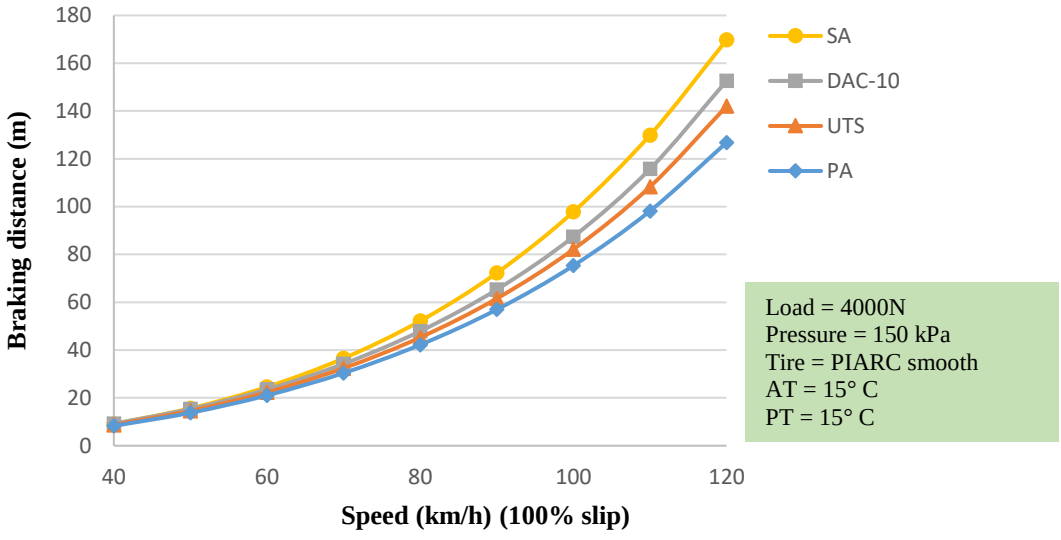

(a)

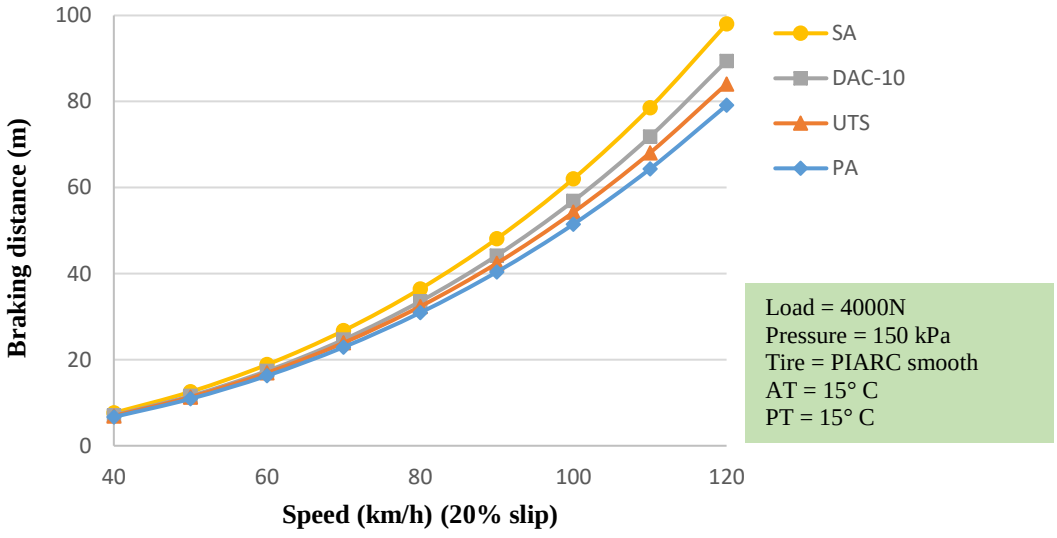

(b)

FIGURE 7 Schematic of influence of asphalt mix design on braking distance

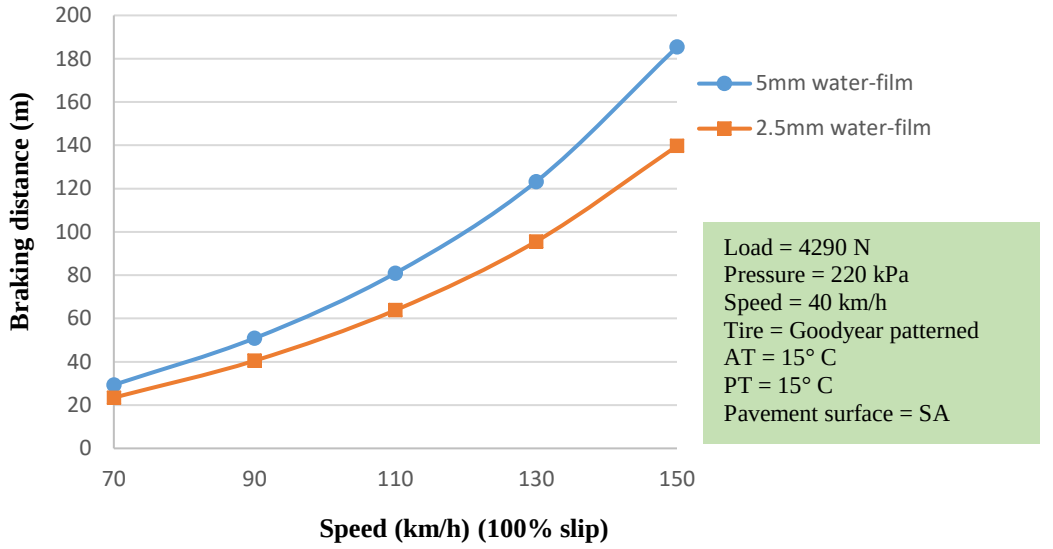

(a)

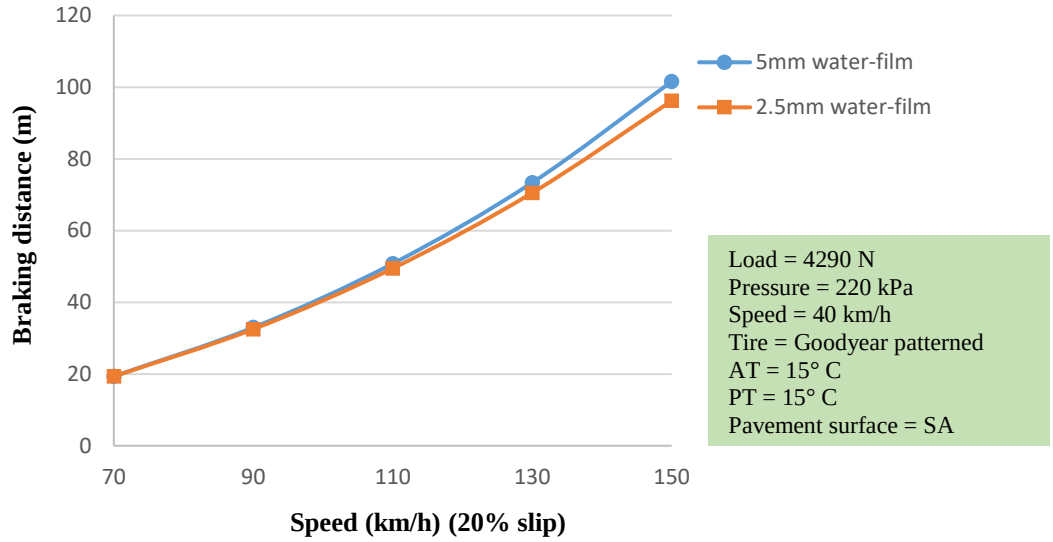

(b)

FIGURE 8 Schematic of influence of water film thickness on braking distance

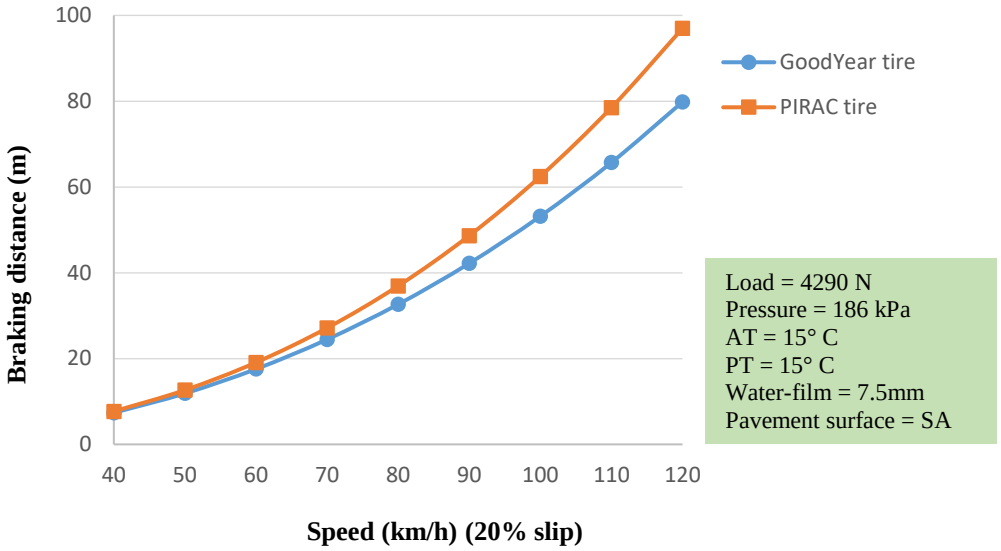

(a)

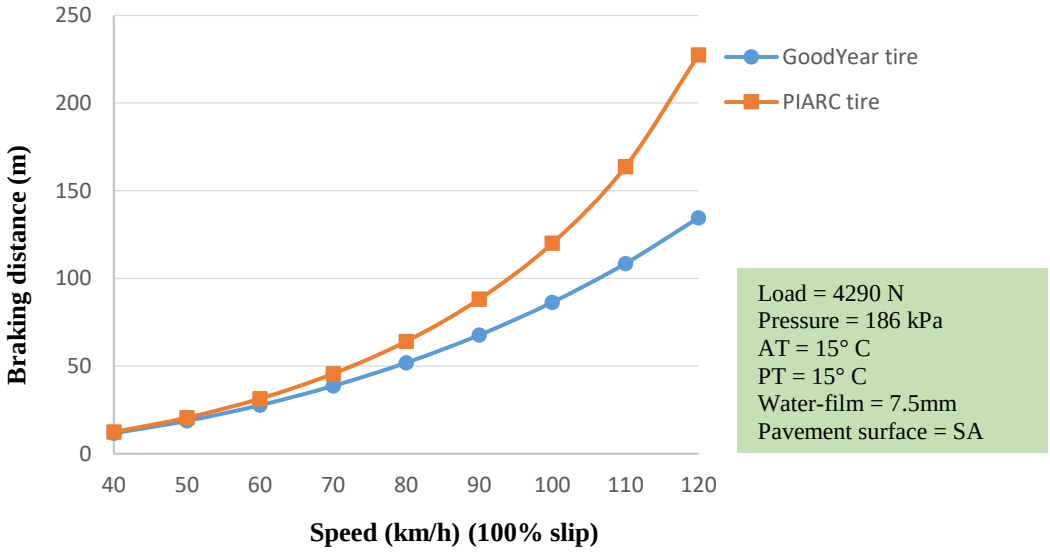

(b)

FIGURE 9 Schematic of influence of tire type on braking distance

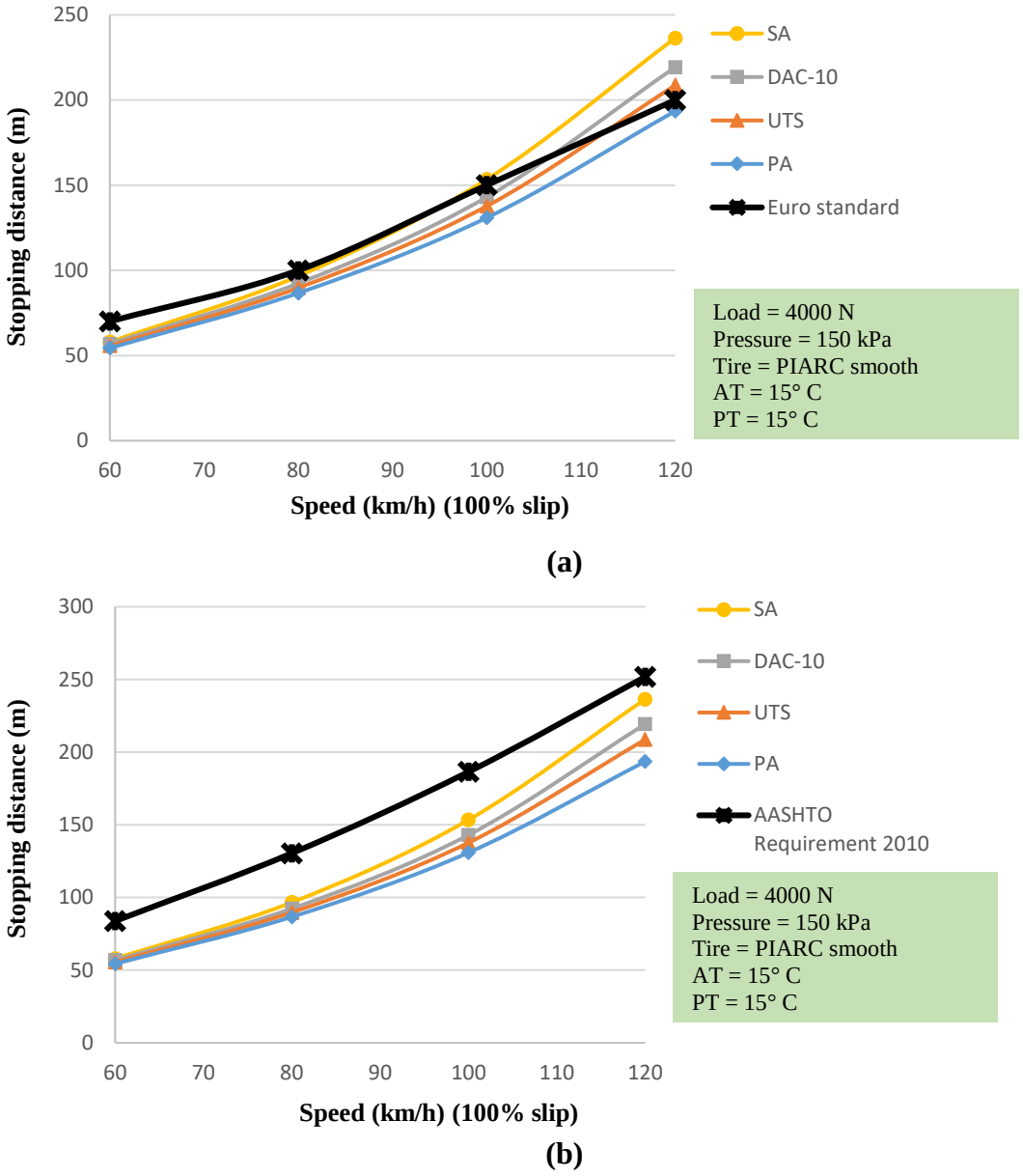

FIGURE 10 Schematic of the comparison on braking distance with Euro standard and AASHTO Requirement 2010